1st Collaboration-ready Draft (Includes Pre-reader Comments):

A Precision Measurement of the Beam-Normal Single-Spin Asymmetry in Forward-Angle Elastic Electron-Proton Scattering

D. Androić,[1] D.S. Armstrong,[2,*] A. Asaturyan,[3] J. Balewski,[4] K. Bartlett,[2] J. Beaufait,[5] R.S. Beminiwattha,[6,7] J. Benesch,[5] F. Benmokhtar,[8] J. Birchall,[9] R.D. Carlini,[5,10] J.C. Cornejo,[2] S. Covrig Dusa,[5] M.M. Dalton,[11,5] C.A. Davis,[12] W. Deconinck,[2] J. Diefenbach,[13] J.F. Dowd,[2] J.A. Dunne,[14] D. Dutta,[14] W.S. Duvall,[15] M. Elaasar,[16] W.R. Falk,[9,†] J.M. Finn,[2,†] T. Forest,[17,7] C. Gal,[11] D. Gaskell,[5] M.T.W. Gericke,[9] J. Grames,[5] V.M. Gray,[2] K. Grimm,[7,2] F. Guo,[4] J.R. Hoskins,[2] D. Jones,[11] M.K. Jones,[5] R.T. Jones,[18] M. Kargiantoulakis,[11] P.M. King,[6] E. Korkmaz,[19] S. Kowalski,[4] J. Leacock,[15] J.P. Leckey,[2] A.R. Lee,[15] J.H. Lee,[6,2] L. Lee,[12,9] S. MacEwan,[9] D. Mack,[5] J.A. Magee,[2] R. Mahurin,[20] J. Mammei,[9,15] J.W. Martin,[21] M.J. McHugh,[22] D. Meekins,[5] J. Mei,[5] K.E. Mesick,[22,23] R. Michaels,[5] A. Micherdzinska,[22] A. Mkrtchyan,[3] H. Mkrtchyan,[3] N. Morgan,[15] A. Narayan,[14] L.Z. Ndukum,[14] V. Nelyubin,[11] Nuruzzaman,[13,14] W.T.H van Oers,[12,9] V.F. Owen,[2] S.A. Page,[9] J. Pan,[9] K.D. Paschke,[11] S.K. Phillips,[24] M.L. Pitt,[15] M. Poelker,[5] R.W. Radloff,[6] J.F. Rajotte,[4] W.D. Ramsay,[12,9] J. Roche,[6] B. Sawatzky,[5] T. Seva,[25] M.H. Shabestari,[14] R. Silwal,[11] N. Simicevic,[7] G.R. Smith,[5] P. Solvignon,[5,†] D.T. Spayde,[26] A. Subedi,[14] R. Subedi,[22] R. Suleiman,[5] V. Tadevosyan,[3] W.A. Tobias,[11] V. Tvaskis,[21] B. Waidyawansa,[6] P. Wang,[9] S.P. Wells,[7] S.A. Wood,[5] S. Yang,[2] P. Zang,[27] and S. Zhamkochyan[3]

(The Q_{weak} Collaboration (Author list to be confirmed)

[1] *University of Zagreb, Zagreb, HR 10002 Croatia*
[2] *William & Mary, Williamsburg, VA 23185 USA*
[3] *A. I. Alikhanyan National Science Laboratory (Yerevan Physics Institute), Yerevan 0036, Armenia*
[4] *Massachusetts Institute of Technology, Cambridge, MA 02139 USA*
[5] *Thomas Jefferson National Accelerator Facility, Newport News, VA 23606 USA*
[6] *Ohio University, Athens, OH 45701 USA*
[7] *Louisiana Tech University, Ruston, LA 71272 USA*
[8] *Duquesne University, Pittburgh, PA 15282, USA*
[9] *University of Manitoba, Winnipeg, MB R3T2N2 Canada*
[10] *William and Mary, Williamsburg, VA 23185 USA*
[11] *University of Virginia, Charlottesville, VA 22903 USA*
[12] *TRIUMF, Vancouver, BC V6T2A3 Canada*
[13] *Hampton University, Hampton, VA 23668 USA*
[14] *Mississippi State University, Mississippi State, MS 39762 USA*
[15] *Virginia Polytechnic Institute & State University, Blacksburg, VA 24061 USA*
[16] *Southern University at New Orleans, New Orleans, LA 70126 USA*
[17] *Idaho State University, Pocatello, ID 83209 USA*
[18] *University of Connecticut, Storrs-Mansfield, CT 06269 USA*
[19] *University of Northern British Columbia, Prince George, BC V2N4Z9 Canada*
[20] *Middle Tennessee State University, Murfreesboro, TN 37132 USA*
[21] *University of Winnipeg, Winnipeg, MB R3B2E9 Canada*
[22] *George Washington University, Washington, DC 20052 USA*
[23] *Rutgers, the State University of New Jersey, Piscataway, NJ 088754 USA*
[24] *University of New Hampshire, Durham, NH 03824 USA*
[25] *Department of Physics, University of Zagreb, Zagreb, HR 10002 Croatia*
[26] *Hendrix College, Conway, AR 72032 USA*
[27] *Syracuse University, Syracuse, NY 13244 USA*

(Dated: May 26, 2020)

A beam-normal single-spin asymmetry generated in the scattering of transversely polarized electrons from unpolarized nucleons is an observable related to the imaginary part of the two-photon exchange process. We report a 2% precision measurement of beam-normal single-spin asymmetry in elastic electron-proton scattering with a mean scattering angle of $\theta = 7.9^\circ$ and a mean energy of 1.149 GeV. The asymmetry result is $B_n = -5.194 \pm 0.067$ (stat) ± 0.082 (syst) ppm. This is the most precise measurement of this quantity available to date and therefore provides a stringent test of two-photon exchange models at $\theta \to 0$ where they should be most reliable.

PACS numbers: 25.30.Bf,13.60.Fz,24.70.+s

The high intensities of electron beams at facilities like Jefferson Lab, MAMI, and the future EIC make them

ideal for studying the charge and magnetization distributions inside nuclear matter in the single-photon exchange approximation. However, measurements with high precision can be affected by two-photon exchange (TPE). Depending on the observable, either the real or imaginary part of the TPE amplitude can play a role.

There has been significant effort to study the real part of the TPE amplitude because it affects cross sections. However, the uncertainties in the theoretical calculations are large, and constraints on models remain weak even after a decade-long program of targeted measurements [1]. An alternative approach is to study observables proportional to the imaginary part of the TPE amplitude such as the beam-normal single-spin asymmetry (BNSSA, or just B_n) .

B_n is a parity- and CP-conserving asymmetry typically at the few part-per-million (ppm) level for forward angles and GeV-scale incident energies in $\vec{e}p$ elastic scattering. Required by time-reversal invariance to vanish in the one-photon exchange (Born) approximation, a non-zero B_n can only arise with the exchange of two or more photons between the scattered electron and the target nucleon [2].

Experimentally, B_n manifests itself as the amplitude of an azimuthal variation in the asymmetry measured when the beam is polarized transverse to its incident momentum.

Theoretically, two complementary approaches have been pursued. One [3, 4] is expected to be valid at all angles, but should work best at lower energies because it only includes the πN intermediate state as well as the (smaller) elastic contribution. The other approach [1, 2, 5–10] is expected to work at all energies because it includes contributions from multi-particle intermediate states (e.g. $\pi\pi$N, ηN, KΛ, ...), but works best at forward angles because it uses the optical theorem to relate the measured total photoproduction cross-section to the imaginary part of the TPE forward scattering amplitude $\mathcal{I}m$(TPE).

TPE was generally treated as small (percent-level) corrections to the unpolarized scattering cross-section which are independent of hadronic structure [11, 12]. However in 2000 a striking disagreement in the proton's elastic electromagnetic form-factor ratio (G_E^p/G_M^p) was observed when comparing Rosenbluth (L/T) separation [13] and polarization transfer [14] results at $Q^2 \geq 2$ (GeV/c)^2. This discrepancy (known as the proton form-factor puzzle) could be explained [15] by a correction involving the real part of the TPE amplitude which modifies the Rosenbluth cross-section, but largely cancels in the polarization-transfer ratios. A recent summary can be found in [1].

The real part of the TPE amplitude $\mathcal{R}e$(TPE) can be determined from the ratio of $e^{\pm}p$ cross sections (see VEPP-3 [16], OLYMPUS [17], CLAS [18]). In principle $\mathcal{R}e$(TPE) can also be determined from the imaginary part via dispersion relations. In practice this is difficult since a broad range of kinematics is needed and there is a paucity of B_n results. Nevertheless, the effects of TPE on the proton radius puzzle (see [19] for the most recent results and a summary) have been explored theoretically [6] using an unsubtracted fixed-t dispersion relation to do just that, predicting that TPE effects are at the level of the present uncertainties ($\sim 1\%$) in the proton radius determinations from ep scattering data. Future experiments (MUSE [20, 21]) aim to improve this precision and further explore TPE effects by comparing $e^{\pm}p$ and $\mu^{\pm}p$ scattering. This underscores the importance of providing B_n data to test the predictions of $\mathcal{I}m$(TPE).

The kinematics of this experiment are at a far-forward angle (7.9°) where the optical model approach should work well, and with a small four-momentum transfer $Q^2 = -t = 0.0248$ (GeV/c)^2, and an intermediate energy ($E_{\rm lab} = 1.149$ GeV, $E_{\rm cm} = 1.74$ GeV) where up to five-pion intermediate states can contribute. The asymmetry is generated by the interference of one-photon and two-photon exchange processes and has the form [22]

$$B_n = \frac{\sigma^{\uparrow} - \sigma^{\downarrow}}{\sigma^{\uparrow} + \sigma^{\downarrow}} = \frac{2\,\mathcal{I}m(\mathcal{M}^{\gamma\gamma}\mathcal{M}^{\gamma *})}{|\mathcal{M}^{\gamma}|^2}, \qquad (1)$$

where $\sigma^{\uparrow}(\sigma^{\downarrow})$ denotes the scattering cross section for electrons with spin parallel (anti-parallel) to a vector $\hat{n}$ normal to the scattering plane, where $\hat{n} = (\vec{k} \times \vec{k'})/(|\vec{k} \times \vec{k'}|)$ with $\vec{k}(\vec{k'})$ being the momentum of the incoming(outgoing) electron. $\mathcal{M}^{\gamma}$ and $\mathcal{M}^{\gamma\gamma}$ are the amplitudes for one- and two-photon exchange. For transversely-polarized electrons scattering from unpolarized nucleons, the detected asymmetry then depends on the azimuthal scattering angle ϕ via $A_{\rm exp}(\phi) \approx B_n \vec{P} \cdot \hat{n}$, where $\vec{P}$ is the electron polarization vector.

Companion measurements of B_n are necessary in most parity-violating electron scattering experiments in order to account for the effects of residual transverse polarization in the nominally longitudinally-polarized beam. Previous measurements of B_n at far-forward angles ($6.0° < \theta_{\rm lab} < 9.7°$) were obtained by the G0 [23] and HAPPEX [24] collaborations near $E_{\rm lab} \sim 3$ GeV. Somewhat larger-angle results have been obtained at MAMI [25, 26] for ($\theta_{\rm lab}$, $E_{\rm lab}$) = ($\sim 34°, 0.3 - 1.5$ GeV), and by SAMPLE [27] at ($\sim 55°, 0.2$ GeV). Backward angle experiments were performed at ($108°, 0.36$ & 0.69 GeV) by G0 [28], and at ($145°, 0.32$ & 0.42 GeV) by PVA4 [29]. Some of these experiments also included results on deuterium [28, 29] as well as heavier nuclei [24].

The ($7.9°, 1.149$ GeV) elastic $\vec{e}p$ B_n measurement reported here was part of a series of ancillary/companion measurements performed by the $Q_{\rm weak}$ collaboration to constrain systematic uncertainties in the first determination of the weak charge of the proton [30, 31]. The general performance of the experimental apparatus is described in Ref. [32]. Details relevant to the extraction of B_n are presented here.

A total of 54 hours of B_n data were collected in three measurement periods and with two different orientations of transverse polarization. Polarized electrons were generated by photo-emission from a strained GaAs cathode at the injector of the Thomas Jefferson National Accelerator Facility. Two Wien filters [33] were used to rotate the electron spin in the transverse plane to horizontal (spin pointing to beam-right at the target) or vertical (spin pointing up). The transversely polarized, 150 μA - 180 μA electron beam was then accelerated to 1.16 GeV before reaching the Q_{weak} apparatus in the experimental Hall C and scattering from unpolarized liquid hydrogen encased in a 34.4-cm-long aluminum-alloy cell with thin (0.1 mm thick) windows where the beam entered and exited. Longitudinal polarization measurements (bracketing the transverse running) using Møller and Compton polarimeters [34–36] upstream of the target yielded an average statistics-weighted beam polarization $\langle P \rangle = (88.72 \pm 0.70)\%$. During the transverse running, the polarization was verified to be transverse via null measurements with the Moller polarimeter, which is only sensitive to longitudinal beam polarization. A set of collimators located downstream of the target selected electrons with lab scattering angles of 5.8° to 11.6°. A toroidal magnet then focused elastic electrons onto a set of eight Cherenkov detectors placed symmetrically around the beam axis, 12.2 m downstream of the target. The azimuthal coverage of the detector array was 49% of 2π.

The spin direction of the electrons was selected from one of two pseudo-randomly chosen ↑↓↓↑ or ↓↑↑↓ quartet patterns generated at 240 Hz. Here ↑ represents the standard spin orientation (spin up or to beam right) and ↓ represents a 180° rotation in the corresponding plane. The signals from the Cherenkov detectors were integrated for each ↑ and ↓ spin state (at 960 Hz). The detector asymmetries were calculated for each quartet using $A_{\rm raw} = \frac{Y_\uparrow - Y_\downarrow}{Y_\uparrow + Y_\downarrow}$ where $Y_{\uparrow\downarrow}$ is the charge-normalized detector yield in the ↑ or ↓ spin state. The systematic uncertainty due to the beam charge normalization was negligible here [30]. False asymmetries from spin-correlated beam position, angle, and energy changes were largely cancelled by the periodic insertion of a half-wave plate (IHWP) located in the injector. The remaining false asymmetries were removed using $A_{\rm msr} = A_{\rm raw} - \sum_{i=1}^{5} \left(\frac{\partial A}{\partial \chi_i}\right) \Delta\chi_i$ where $\Delta\chi_i$ are the helicity-correlated differences in beam trajectory or energy over the helicity quartet, and the slopes $\partial A/\partial\chi_i$ were determined using multi-variable linear regression. False asymmetries caused by secondary events scattered from beamline elements were negligible [30].

The measured asymmetries $A^i_{\rm msr}$ in detector i, for both orientations of the transverse beam polarization, were fit to

$$A^i_{\rm msr}(\phi_i) = R_l R_{\rm av} A_{\rm exp} \sin(\phi_{\rm s} - \phi_i + \phi_{\rm off}) + C, \qquad (2)$$

to extract the experimental asymmetry $A_{\rm exp}$. Here ϕ_s is the azimuthal angle of $\vec{P}$, and ϕ_i is the azimuthal angle of the i^{th} detector in the plane normal to the beam axis. The factor $R_{\rm av} = 0.9938 \pm 0.0006$ accounts for the averaging of the asymmetry over the effective azimuthal acceptance ($\approx 22°$) of a Cherenkov detector and $R_l = 1.007 \pm 0.005$ corrects for the measured non-linearity in the detector electronics. A floating offset in phase $\phi_{\rm off}$ was included to account for any detector offsets in the azimuthal plane, and a floating constant C was included to represent any monopole asymmetries, such as due to parity-violating asymmetry generated by any residual longitudinal beam polarization. The fitted values for $\phi_{\rm off}$ and C were consistent with zero, and the value of $A_{\rm exp}$ extracted was insensitive to the inclusion of these extra fit parameters.

The fits to Eq. 2 for two of the three data sets are shown in Fig. 1. Since the kinematics were similar and the results consistent, the error-weighted average of the three measurements $A_{\rm exp} = -4.801 \pm 0.056$ (stat) ± 0.039 (syst) ppm was used as the experimental asymmetry from the full measurement. The systematic error accounts for the uncertainties in R_l, R_{av} and the linear regression.

The experimental asymmetry $A_{\rm exp}$ was then corrected for backgrounds. The largest background was $f_1 = 3.3 \pm 0.2\%$, a dilution from elastic and quasi-elastic electrons scattering from the aluminum-alloy beam-entrance and exit windows of the target. Dedicated measurements using an aluminum-alloy target, similar to but thicker than the windows used in the target cell, were used to determine the aluminum asymmetry A_1 [37]. Another background correction was applied for $f_2 = 0.018 \pm 0.004\%$, a dilution due to inelastic electrons. The inelastic asymmetry A_2 [37] was determined using dedicated measurements with the toroidal magnet configured to focus inelastic electrons onto the detectors. Addition-

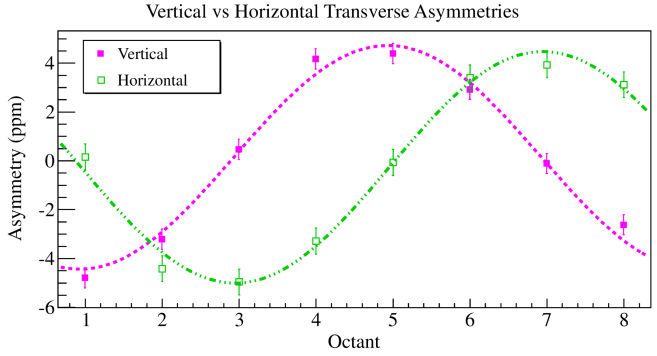

FIG. 1. Extraction of the experimental asymmetry $A_{\rm exp}$ from the measured asymmetries $A^i_{\rm msr}$ for two of the data sets. The octant number corresponds to the azimuthal location of the detectors, starting from beam left (Octant 1) where ϕ_i=0, and going clockwise. The reduced χ^2 in the vertical and horizontal fits are 1.4 and 0.9, respectively.

ally, neutral backgrounds in the acceptance generated by sources in the beamline ($f_3 = 0.19 \pm 0.06\%$ dilution) and other sources ($f_4 < 0.3\%$ dilution) were studied. These neutral backgrounds constituted negligible corrections to the experiment's final azimuthal asymmetry. Therefore, no correction was applied ($A_3 \approx A_4 \approx 0$). However, their dilutions were taken into consideration.

A unique potential background asymmetry not yet observed in a B_n measurement is a parity-violating beam-transverse single-spin asymmetry (B_t), generated by the interference between one-photon exchange and the Z^0-exchange processes. At our kinematics, B_t is estimated to be on the order of 10^{-11} [38], too small to be observed in this experiment.

The various corrections were applied to the experimental asymmetry $A_{\rm exp}$ to extract B_n following

$$B_n = R_{\rm tot}\left[\frac{A_{\rm exp}/P - \sum_{i=1}^{4} f_i A_i}{1 - \sum_{i=1}^{4} f_i}\right] + A_{\rm bias}. \qquad (3)$$

Here A_i is the background asymmetry generated by the i^{th} background (aluminum windows, inelastics, beamline neutrals, and other neutrals, respectively) with dilution f_i. The factor $R_{\rm tot} = 1.0041 \pm 0.0046$ accounts for electron energy-loss and depolarization from electromagnetic radiation, non-uniform Q^2 distribution across the detectors, light-collection variation across the detectors, and the uncertainty in the acceptance-averaged $\langle Q^2 \rangle = 0.0248 \pm 0.0001$ GeV^2. $A_{\rm bias} = 0.125 \pm 0.041$ ppm is a false asymmetry that arose due to the analyzing power of the scattered electrons which can rescatter in the lead preradiators installed upstream of each main detector. This effect is described in detail elsewhere [30]; it was larger in magnitude in the present case because, for transversely polarized beam, it does not largely cancel due to the symmetry of the apparatus. With the above corrections, we obtain a value of $B_n = -5.194 \pm 0.067$ (stat) $\pm$ 0.082 (syst) ppm for elastic electron-proton scattering at a vertex scattering angle of $\langle \theta \rangle = 7.9^\circ$ and vertex energy $\langle E \rangle = 1.149$ GeV. The contributions from different error sources are summarized in Table I and discussed in more detail in Ref. [37].

Figure 2 compares our measurement to three model calculations: Pasquini & Vanderhaeghen [3, 4], Afanasev & Merenkov [9, 10] and Gorchtein [2, 5–8]. One calculation [2, 5–8] is in reasonable agreement with this measurement (within 0.3 ppm, or just 6%, but still 2.6 σ away, given the small $Q_{\rm weak}$ uncertainty). The other group [9, 10] which also makes use of the optical theorem is only slightly further away. The Pasquini & Vanderhaeghen model significantly underpredicts the magnitude of B_n. The latter calculation uses unitarity to model the Doubly Virtual Compton Scattering (VVCS) tensor in the resonance regime in terms of electroabsorption amplitudes whereas both Afanasev & Merenkov as well as Gorchtein use the optical theorem to relate the forward VVCS tensor to the total photoabsorption cross section. Although the three calculations predict similar angular behavior for the asymmetry in our acceptance, their normalizations vary widely.

Generally, the models agree that the dominant contribution to the asymmetry comes from the inelastic intermediate states of the nucleon in TPE. The con-

TABLE I. Summary of experimental uncertainties.

Uncertainty Source	$\frac{\Delta B_n}{B_n}$ (%)
Statistics	1.29
Systematics	
P: Beam polarization	0.807
R_{tot}: Kinematics and acceptance	0.428
R_l: Electronic Non-linearity	0.540
Linear regression	0.656
R_{av}: Acceptance averaging	0.067
A_1: Aluminum background asymmetry	0.408
f_1: Aluminum dilution	0.172
A_2: Inelastic background asymmetry	0.024
f_2: Inelastic dilution	0.030
A_3: Beamline neutral asymmetry	0.004
f_3: Beamline neutral dilution	0.064
A_4: Other neutral background asymmetry	0.201
f_4: Other neutral background dilution	0.213
$A_{\rm bias}$	0.789
Systematics Sub Total	1.57
Total Uncertainty	2.03

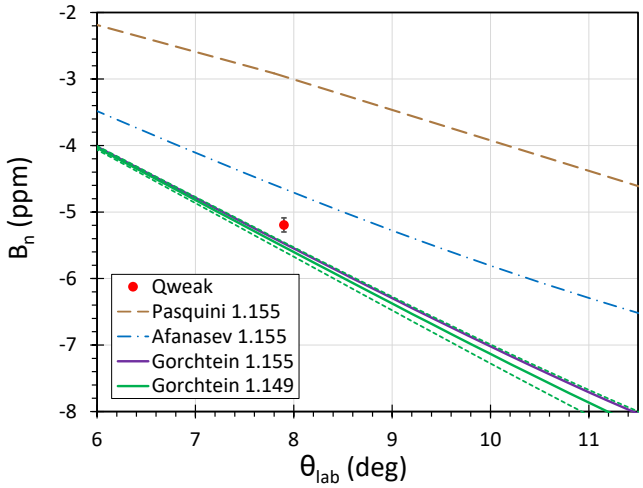

FIG. 2. Comparison of this measurement (red circle) to calculations at $E_{\rm lab}$=1.155 GeV by Pasquini & Vanderhaeghen [3], Afanasev & Merenkov [9], and Gorchtein [5] over the $Q_{\rm weak}$ acceptance. The latter calculation is also shown at 1.149 GeV (the $Q_{\rm weak}$ energy), along with the uncertainties associated with that calculation (dashed green lines).

tribution from the elastic state is insignificant. However, both the Afanasev & Merenkov model and the Gorchtein model consider all inelastic intermediate states with multi-pion excitations whereas the Pasquini & Vanderhaeghen model only considers inelastic states with single-pion excitations. This likely causes the largest difference between the two types of calculations.

The calculations from the three theoretical groups discussed here differ at different kinematics, making a global comparison to other experiments difficult. For example, the Gorchtein model includes corrections to account for the off-forward 34° data of [26], which are not used to predict the far-forward 7.9° kinematics of this experiment. However, it is still instructive to compare the existing forward angle B_n data to the kinematics-specific predictions from each theoretical group. Such a comparison is shown as a function of $E_{\rm lab}$ in Figure 3 for $\theta_{\rm lab} \leq 34°$ data. This figure shows that all the models have significant disagreements with the less-forward angle ($\theta_{lab} > 10°$) data. The far-forward data are in a better position to be described theoretically using the optical theorem and those calculations do show reasonable agreement. The $Q_{\rm weak}$ result provides by far the most precise test of models to date in the kinematic region where they are expected to be most accurate.

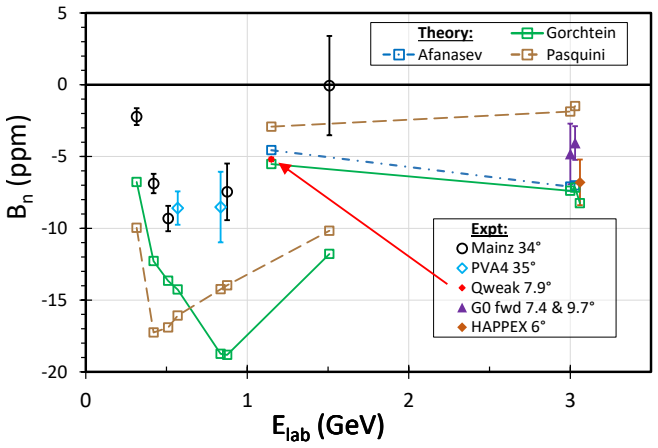

FIG. 3. Energy dependence of all forward-angle ($\theta_{\rm lab} \leq 34°$) elastic $\vec{e}p$ B_n data compared to calculations at each experiment's kinematics. The predictions (open squares) from each theoretical group (Pasquini & Vanderhaeghen [3, 4], Afanasev & Merenkov [9, 10], and Gorchtein [5, 8]) are broken into separate lines for the far-forward and the forward angle data, to help guide the eye. The far-forward angle data (solid circles, $\theta_{\rm lab} < 10°$) are from this experiment (red, uncertainties smaller than the symbol), G0 (purple), and HAPPEX (orange). Less forward-angle data $\theta_{\rm lab} \sim 34°$ are denoted with open circles from MAMI (black) and PVA4 (cyan).

The beam-normal single-spin asymmetry is a unique tool to test dispersion relations used in calculating TPE corrections to ep scattering cross sections. In light of improving these TPE corrections in ep and μp scattering observables, precision measurements of B_n are extremely useful for validating TPE models. The precise $Q_{\rm weak}$ datum reported here, in particular, provides a stringent test of the TPE models at far-forward angles and moderate energy.

This work was supported by DOE Contract No. DEAC05-06OR23177, under which Jefferson Science Associates, LLC operates Thomas Jefferson National Accelerator Facility. Construction and operating funding for the experiment was provided through the U.S. Department of Energy (DOE), the Natural Sciences and Engineering Research Council of Canada (NSERC), and the National Science Foundation (NSF) with university matching contributions from the College of William and Mary, Virginia Tech, George Washington University, and Louisiana Tech University. We wish to thank the staff of Jefferson Lab, TRIUMF, and MIT Bates, as well as our undergraduate students, for their vital support during this challenging experiment. We would like to thank B. Pasquini, A. Afanasev, M. Gorchtein, M. Vanderhaeghen, O. Tomalak, P. Blunden and W. Melnitchouk for useful discussions.

* corresponding author: armd@jlab.org
† deceased

[1] A. Afanasev, P. Blunden, D. Hasell, and B. Raue, Prog. Part. Nucl. Phys. **95**, 245 (2017), arXiv:1703.03874 [nucl-ex].
[2] M. Gorchtein, P. A. Guichon, and M. Vanderhaeghen, Nucl.Phys. **A741**, 234 (2004).
[3] B. Pasquini and M. Vanderhaeghen, Phys.Rev. **C70**, 045206 (2004).
[4] B. Pasquini, private communication.
[5] M. Gorchtein, Phys.Rev. **C73**, 055201 (2006).
[6] M. Gorchtein, Phys. Rev. C **90**, 052201 (2014), arXiv:1406.1612 [nucl-th].
[7] M. Gorchtein, P. Guichon, and M. Vanderhaeghen, Nuclear Physics A **741**, 234 (2004).
[8] M. Gorchtein, private communication.
[9] A. V. Afanasev and N. Merenkov, Phys.Lett. **B599**, 48 (2004).
[10] A. Afanasev, private communication.
[11] L. W. Mo and Y.-S. Tsai, Rev. Mod. Phys. **41**, 205 (1969).
[12] L. Maximon and J. Tjon, Phys.Rev. **C62**, 054320 (2000).
[13] M. Rosenbluth, Phys.Rev. **79**, 615 (1950).
[14] M. Jones *et al.* (Jefferson Lab Hall A Collaboration), Phys.Rev.Lett. **84**, 1398 (2000).
[15] P. A. Guichon and M. Vanderhaeghen, Phys.Rev.Lett. **91**, 142303 (2003).
[16] I. A. Rachek *et al.*, Phys. Rev. Lett. **114**, 062005 (2015).
[17] B. S. Henderson *et al.* (OLYMPUS), Phys. Rev. Lett. **118**, 092501 (2017).
[18] D. Adikaram *et al.* (CLAS), Phys. Rev. Lett. **114**, 062003 (2015).
[19] W. Xiong *et al.*, Nature **575**, 147 (2019).

[20] R. Gilman *et al.* (MUSE), (2013), arXiv:1303.2160 [nucl-ex].

[21] R. Gilman *et al.* (MUSE), (2017), arXiv:1709.09753 [physics.ins-det].

[22] A. De Rujula, J. Kaplan, and E. De Rafael, Nucl.Phys. **B35**, 365 (1971).

[23] D. S. Armstrong *et al.* (G0 Collaboration), Phys.Rev.Lett. **99**, 092301 (2007).

[24] S. Abrahamyan *et al.* (HAPPEX, PREX), Phys. Rev. Lett. **109**, 192501 (2012), arXiv:1208.6164 [nucl-ex].

[25] F. E. Maas *et al.*, Phys. Rev. Lett. **94**, 082001 (2005), arXiv:nucl-ex/0410013 [nucl-ex].

[26] B. Gou *et al.*, Phys. Rev. Lett. **124**, 122003 (2020), arXiv:2002.06252 [nucl-ex].

[27] S. P. Wells *et al.* (SAMPLE), Phys. Rev. **C63**, 064001 (2001), arXiv:nucl-ex/0002010 [nucl-ex].

[28] D. Androic *et al.* (G0), Phys. Rev. Lett. **107**, 022501 (2011), arXiv:1103.3667 [nucl-ex].

[29] D. B. Ríos *et al.*, Phys. Rev. Lett. **119**, 012501 (2017).

[30] D. Androic *et al.* ($Q_{\rm weak}$ Collaboration), Nature **557**, 207 (2018).

[31] D. Androic *et al.* (Q_{weak} Collaboration), Phys. Rev. Lett. **111**, 141803 (2013).

[32] T. Allison *et al.* ($Q_{\rm weak}$ Collaboration), Nucl. Instrum. Methods **A781**, 105 (2015).

[33] J. James, P. Adderley, J. Benesch, J. Clark, J. Hansknecht, *et al.*, in *Proc. of 2011 Particle Accelerator Conf.* (New York, NY, 2011).

[34] M. Hauger *et al.*, Nucl. Instrum. Methods **A462**, 382 (2001).

[35] J. A. Magee *et al.*, Phys. Lett. **B766**, 339 (2017).

[36] A. Narayan *et al.*, Phys. Rev. **X6**, 011013 (2016).

[37] D. B. P. Waidyawansa, *A 3% Measurement of the Beam Normal Single Spin Asymmetry in Forward Angle Elastic Electron Proton Scattering Using the Q_{weak} Setup*, Ph.D. thesis, Ohio University (2013).

[38] W. Melnitchouk, P. Blunden, and P. Sachdeva, private communication.